Nanoscale

Accepted Manuscript

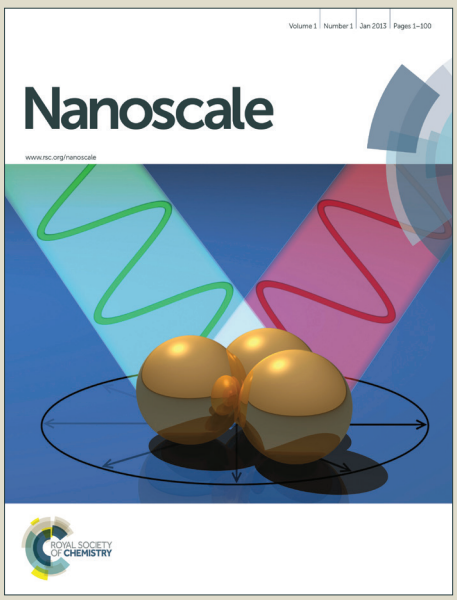

ROYAL SOCIETY OF CHEMISTRY

www.rsc.org/nanoscale

High-Performance Moisture Sensor based on Ultralarge Graphene Oxide

Boon-Hong Wee,[a] *Wai-Hwa Khoh*,[a] *Ashis K. Sarker*,[b] *Chang-Hee Lee*,[b] *and Jong-Dal Hong*[a]*

[a] Department of Chemistry, Research Institute of Natural Sciences, Incheon National University, 119 Academy-ro, Yeonsu-gu, Incheon, 406-772, Republic of Korea.

[b] Department of Electrical and Computer Engineering, Seoul National University, Seoul 151-742, Republic of Korea

*To whom all correspondence should be addressed.

E-mail: hong5506@inu.ac.kr

Keywords: Ultralarge Graphene Oxide, Fingertip Moisture, Humidity Sensor, Ultrahigh Sensitivity, Response/Recovery Time

ABSTRACT

This article describes the effect of the lateral size of graphene oxide (GO) on the humidity sensing properties of a GO-based sensor. The GO size effect on the humidity sensing performance was evaluated on gold electrodes drop-coated with either ultralarge graphene oxide UGO (lateral size = 47.4 ± 22.2 μm) or small-size graphene oxide SGO sheets (lateral size = 0.8 ± 0.5 μm). The in-plane conductance obtained from the UGO and SGO electrodes was found to increase by four orders of magnitude and by three orders of magnitude, respectively, upon exposure to relative humidity RH change from 7 to 100 %. The maximal sensitivity (*S*) values of the UGO and SGO humidity sensors were determined to be S_{UGO} = 4339 ± 433 and S_{SGO} = 1982 ± 122. The GO size clearly influenced the overall proton conductivity, as evidenced by the activation enthalpy (E_a) required for proton conduction in UGO and SGO sheets: E_a (UGO) = 0.63 eV, E_a (SGO) = 1.14 eV. The UGO humidity sensor exhibited an excellent device

performance with a high sensitivity and an ultrafast response/recovery time (0.2/0.7 s). Good humidity sensing stability was observed, with a variation of only ±4.6% over five days. The resistive-type UGO humidity sensor was capable of sensing the moisture on a fingertip at a distance of 0.5 mm with a sensitivity of 17.4 and a response/recovery time of 0.6 s/1.3 s. The excellent device performance of the UGO humidity sensor also permitted the determination of the position of a fingertip by detecting the fingertip moisture, hence offering a great potential for touchless display position interface applications.

1. Introduction

Humidity sensors are critical in a wide range of applications in the automotive, biomedical, chemical, and electronics industries, as well as in scientific research laboratories.[1,2] These sensors are commonly found in precision air conditioning controls for electronic appliances, breathing air systems, and moisture alarms for pressurized telecommunications transmission cables. The humidity sensing materials in most commercial humidity sensors are composed of either inorganic- or organic-based sensing materials[2] that provide precise measurements of the environmental moisture levels. Inorganic-based sensing materials (i.e. Al_2O_3, In_2O_3, $MnWO_4$, SiO_2, SnO_2, TiO_2, WO_3, and $ZrTiO_3$) are highly sensitive to moisture, and they have limited utility in microchip fabrication industries due to their demand for high processing temperatures (1000 ^oC), which are not compatible with semiconductor manufacturing processes.[2] Several trials have been attempted to replace these inorganic materials with highly soluble organic or polymer-based sensing materials (i.e. polyvinyl alcohol, poly(dimethyldiallyammonium chloride), poly(sodium *p*-styrene sulfonate), poly(vinylpyrrolidone), polyaniline and their corresponding derivatives),[1] which are solution-processable at low temperatures. In some cases, the high solubility of these organic materials in

water presents a major disadvantage, especially when these polymeric materials are intended for use in high humidity conditions.[2] Another critical drawback of most commercial resistive sensors is their relatively slow response time, ranging typically from 10 s to 30 s. Some cheap humidity sensors provide impractically long response time of over 1-2 minutes.[3] Thus, these sensors are not suitable for use as integrated component in wearable and mobile electronics applications, which would require high sensitivity, fast response, and high energy efficiency. In an effort to design better humidity sensors, concerted efforts have been applied toward the development of high performance sensing materials to meet the needs of high-end next generation innovative products.

Graphene oxide (GO) is an excellent amphiphilic soft material due to the presence of various oxygenated functional groups attached to its basal plane and sheet edges.[4,5] These oxygenated functional groups enable the use of GO in proton conductor applications.[6] Despite various experimental and theoretical works on GO, the moisture-sensing mechanism associated with the oxygenated moieties in GO remains the subject of debate.[5-12] Some researchers speculated that GO may not exhibit any ionic conductivity.[7] By contrast, other researchers insisted that the epoxide and hydroxyl groups at the basal plane of GO could form an excellent network of proton hopping sites that serve as proton conduction pathway according to Grotthuss mechanism: $H_2O + H_3O^+ \rightarrow H_3O^+ + H_2O$.[5,10,11,13] These assumptions were recently supported by several experimental studies. A humidity sensor composed of reduced GO (rGO),[14,15] graphene quantum dots,[16] and H-doped graphene[17] exhibited only low humidity sensing properties due to a lack of epoxide and hydroxyl groups. By contrast, GO (functionalized with epoxide and hydroxyl groups) has recently been proved to be an invaluable humidity sensing material owing to its large surface-to-volume ratio and high hygroscopicity.[13] The experimental results suggest

that the humidity sensing properties of GO can be improved significantly by enlarging the GO size, which would increase the effective length of proton conduction pathway (defined as the distance a proton can move without slowing or encountering a break at the boundary of the GO sheets).

This article investigates the effect of GO lateral size on the performances of a GO-based humidity sensor (i.e. sensitivity, the response/recovery time, stability) comprising a pair of gold electrodes (separated by a 50 μm gap) drop-coated with either ultralarge GO sheet denoted UGO (lateral size = 47.4 ± 22.2 μm) or small-size GO sheet denoted SGO (lateral size = 0.8 ± 0.5 μm). The UGO humidity sensor exhibited excellent device performance with high sensitivity (4339 ± 433), ultrafast response/recovery time (0.2/0.7 s), and a good stability with variations of only ±4.6% over five days. The resistive-type UGO humidity sensor was investigated for noncontact-mode moisture sensing, which can be applied in touchless position interface applications.

2. Experimental

2.1 Materials. Natural graphite flake (particle size = –10 mesh) was purchased from Alfa Aesar, potassium permanganate from Sigma-Aldrich, fuming nitric acid (93%) from Matsunoen Chemicals Ltd (Japan), ammonium hydroxide (29%) from Mallinckrodt Baker Inc. (NJ, USA), lithium chloride monohydrate (98.2%) from Shinyo Pure Chemicals Co. Ltd. (Japan), and sodium dichromate dihydrate (99.0%) from Junsei Chemical Co. Ltd. (Japan). Concentrated sulfuric acid (95%), hydrogen peroxide (34.5%), hydrochloric acid (35%), and potassium chromate (98.5%) were purchased from Samchun Pure Chemical Co. Ltd (South Korea). Potassium sulfate (99.0%), and magnesium chloride hexahydrate from Oriental Chemical Industry (South Korea). Sodium nitrite (98.0%), sodium hydroxide (97.0%), and sodium chloride

(99.5%) from Daejung Chemicals and Metals. Co. Ltd., (South Korea). All chemicals were of analytical grade and used without further purification. De-ionized (DI) water (18 MΩ cm^{-1}) was used for all experiments including cleaning procedures. Silicon wafer (d = 100 mm, Libby Owens Ford, USA) was cleaned using the piranha solution (H_2SO_4 and H_2O_2; 7:3 ratio) and followed by RCA solution (H_2O, H_2O_2, and NH_4OH; 5:1:1 ratio) for 1 h at 70 °C, respectively, then rinsed with DI water. Transparency PET films purchased from Saehan Industries (South Korea) were cleaned using Digital UV ozone system (PSD Series, Novascan) for 1 h to remove molecular organic contaminations.[18]

2.2 Preparation of Ultralarge Graphene Oxide (UGO) and Small Graphene Oxide (SGO) The precursor GO was synthesized based on the Hummers method using thermally expanded graphite, as described in the Supporting Information (SI).[19] The UGO and SGO dispersions were prepared according to the method reported by Kim *et al*.[20] In brief, the as-prepared GO suspension was diluted with DI water and centrifuged at 8 000 rpm for 40 min in order to collect SGO from the supernatant (SGO). The sediment was redispersed in DI water again and then separated by centrifugation at 4 000 rpm for 40 min, yielding ultralarge graphene oxide (UGO) in the sediment. Later, the UGO was redispersed in DI water. The highest yield of the UGO fraction was relatively low (8.3 wt%).[19]

2.3 Coating of UGO and SGO on Gold Electrodes. A fixed volume (5 μL) of either UGO or SGO dispersion was drop-coated onto two gold electrodes (separated by an inter-electrode gap of 50 μm), which were deposited onto a PET substrate (Figure S1). The UGO and SGO thin films were air-dried overnight prior to evaluation of their humidity sensing properties.

2.4 Characterization Methods. The lateral sizes of the UGO and SGO sheets and the surface morphology of the films were characterized using field emission scanning electron microscope

(FE-SEM) (JEOL JSM-7800F). Surface roughness and film thickness of the UGO and SGO films were measured using atomic force microscopy (AFM) (Park Systems, XE-100). The elemental compositions of the UGO and SGO films were investigated using X-ray photoelectron spectrometer (PHI 5000 VersaProbeII). The structural characteristics of the UGO and SGO films were investigated using Raman spectrometer (Raman-LTPL) with a 532 nm excitation laser.

The DC conductance of the sensors (applied DC voltage of 1 V) at different levels of relative humidity (RH) was measured using Keithley 2400 source meter. The details of the measurement setups were displayed in Figure S1 (SI). The RH was adjusted by bubbling air through saturated salt solutions. The humid air was blown directly over the samples at room temperature (20 ^{o}C) for 30 min.[21] Different types of salt were used to adjust the RH; NaOH.H_2O (7% RH), LiCl.H_20 (11.3% RH), $MgCl_2.6H_2O$ (32.7% RH), $Na_2Cr_2O_7.2H_2O$ (53.7% RH), $NaNO_2$ (64.4% RH), NaCl (75.1% RH), K_2CrO_4 (86.5% RH), and K_2SO_4 (97.0% RH).[21] For 100% RH, DI water was used. The distance between the air nozzle and sample was fixed at 2 mm. In order to calculate the activation enthalpy of proton conduction in UGO and SGO sensor, the AC proton conductivity of the sensors in a humidity chamber (20 ^{o}C, 97 %RH) was measured using an electrochemical impedance spectroscopy (Ivium-StatTechnologies Compactstat) in the frequency range from 1 MHz to 50 Hz with an applied DC voltage of 1 V. The sample was left in the humidity chamber at 20 ^{o}C for 24 h to achieve equilibrium state prior to the measurement. The proton conductivity, σ of the samples was calculated using the formula $\sigma = L/(R \times T \times D)$.[13] The impedance, R was measured from the diameter of the Nyquist plot, which can be obtained by fitting the plot to an equivalent circuit using the ZView program (version 2.3d, Scribner Associates Inc.). The distance between two electrodes, L was fixed for all the samples at 5×10^{-3} cm. The film thickness, T was measured using AFM. The electrode length, D was fixed at 0.3 cm.

3. Results and Discussions

3.1 Microscopic Characterization of UGO and SGO. The lateral sizes of UGO and SGO sheets drop-coated onto a Si/SiO_2 substrate were determined from their respective FE-SEM images, as shown in Figure 1. The average lateral sizes of UGO and SGO sheets were determined to be 47.4 ± 22.2 μm and 0.8 ± 0.5 μm, respectively, based on an analysis of 183 pieces of UGO sheets and 162 pieces SGO sheets, as reported previously (data shown in Figure S2).[19] The lateral size of an UGO sheet could in some cases exceed 150 μm. These large components constituted approximately 7% of the UGO dispersion, and were much larger than the largest components of SGO, which ranged from several hundreds of nanometers to a few micrometers.[22-24]

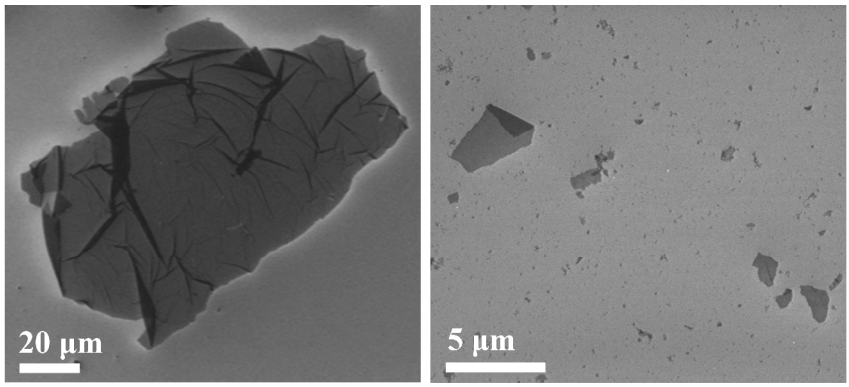

Figure 1. FE-SEM images of UGO (left) and SGO (right). The UGO and SGO sheets were drop-coated using their stable dispersions (5 μL) on a Si/SiO_2 substrate.

3.2 Humidity Sensing Properties of UGO and SGO. The established model of the GO structure, initially proposed by Lerf and Klinowski, stated that the basal plane of GO contains mainly epoxide and hydroxyl groups with small number of carbonyls groups around the hole edges inside the sheet.[25] The sheet edges, by contrast, contain mostly carboxylic acid group.[26] Importantly, a hydroxyl group (bonded to a carbon atom) always accompanied by an epoxide group tethered to an adjacent carbon atom.[27] The epoxide and hydroxyl groups in close

proximity created continuous and well-aligned proton exchange sites on the basal plane of GO, and could be utilized for proton conduction. The proton conduction pathways, however, tended to be blocked by carboxylic acid groups scattered at the edges of the GO sheet.[5,6] Based on the proton conduction mechanism, we predicted that the UGO sheet (with a lateral size of ~ 47 μm) could provide much longer uninterrupted travel distance on the basal plane for proton conduction compared to the travel distances provided by a SGO (with a lateral size < 1 μm), leading to a higher proton conductivity. The energy barrier for proton hopping from one sheet to another at the periphery is expected to be reduced on the larger UGO sheets.[28]

The surface morphologies of the UGO and SGO films were investigated using FE-SEM and AFM, as shown in Figure 2. UGO film exhibited less-wrinkled and flat morphology compared to SGO. A paper by Shen *et al.*[29] reported that the wrinkled structure in the SGO film arose from the edge-to-edge interactions between adjacent individual GO sheets. The sheets within the UGO films were likely to contain fewer edge-to-edge interactions than the sheets within the SGO film, resulting in the formation of a less wrinkled and homogeneous film. The surface roughness (R_a) of UGO (determined from the AFM image analysis) was found to be 9 nm, one-third the value obtained from SGO (R_a = 27 nm) (Figure S3).

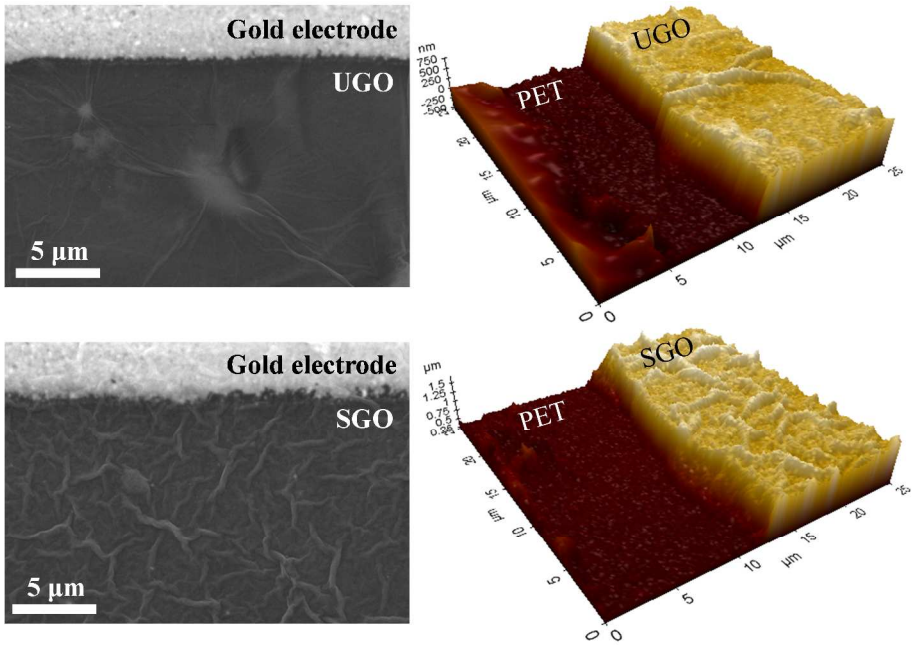

Figure 2. The topographic SEM and AFM images of UGO (top two images) and SGO (bottom two images). The thicknesses of the UGO and SGO were determined to be 617 ± 20 nm and 711 ± 27 nm, respectively.

The sensitivity of the UGO and SGO electrodes (at 20^{o} C) upon exposure to humidity was assessed based on their electrical properties at an applied DC voltage of 1V, as the RH was increased over the range 7 - 100 %, as shown in Figure 3. The UGO and SGO electrodes both displayed a low electrical conductance, (G = 2.8 x 10^{-11} S) at 7% RH (Figure 3a). However, the conductance of UGO increased by four orders of magnitude to 1.2 x 10^{-7} S; whereas the conductance of SGO increased by three orders of magnitude to 5.7 x 10^{-8} S, as RH was switched from 7 to 100 %. The electrical conductance increased exponentially, as the RH increased from 7 to 100 %. This nonlinear stimulus-response characteristics are commonly observed in commercial humidity sensors.[3] The UGO sensor yielded a sensitivity (S) value of 4339 ± 433, and was, therefore, twice as sensitive as the SGO sensor (S = 1982 ± 122). Note that the sensitivity was defined as $S = [G_{100\%RH}-G_{7\%RH}]/G_{7\%RH}$. The UGO electrode exhibited excellent humidity sensitivity, three to four orders of magnitude higher than the sensitivities of sensing

materials reported previously (Table S1 in SI), including H-doped graphene ($S = 0.8$),[17] graphene quantum dots ($S = 0.5$)[16] or reduced graphene oxide ($S = 0.06$).[14] The poor performance of these graphene-based humidity sensors could be explained due to the absence of epoxide and hydroxyl groups on the basal plane of graphene, which are crucial for proton transport. According to Matsumoto *et al*.,[13] the presence of carboxylic acid group at the edge of the reduced GO could also hinder the proton conduction.

The response time and recovery time of the humidity sensors (the time required to reach 90% of the steady state) were determined to be 0.2/0.7 s for the UGO electrode and 0.1/0.3 s for the SGO electrode, respectively, as shown in Figure 3b. The UGO electrode showed slightly slower recovery time compared to the SGO electrode, suggesting that the sizes of the GO sheets did not significantly affect the response and recovery times. It should be noted that the response/recovery time of the highly oxygenated UGO and SGO on humidity sensors were significantly shorter than those obtained from other sensing materials, such as reduced GO (4 s/10 s),[14] graphene quantum dots (10 s/20 s),[16] carbon nanotube (6 s/120 s),[30] SnO_2 (120 s/20 s),[31] or H-doped graphene (3 min/several hours).[17] The UGO resistive-type humidity sensor exhibited high sensitivity (up to 4339 ± 433) with extremely fast response/recovery time (0.1 - 0.2 s). The stability of the UGO and SGO humidity sensors was evaluated based on the DC conductance and the AC conductivity during storage in a humidity chamber (97 %RH, 20 ^{o}C) over a period of five days (Figure 3c,d). The UGO humidity sensor clearly exhibited excellent stability with a variation of only ±4.6% over a period of 5 days, compared to SGO humidity sensor (±48.9%).

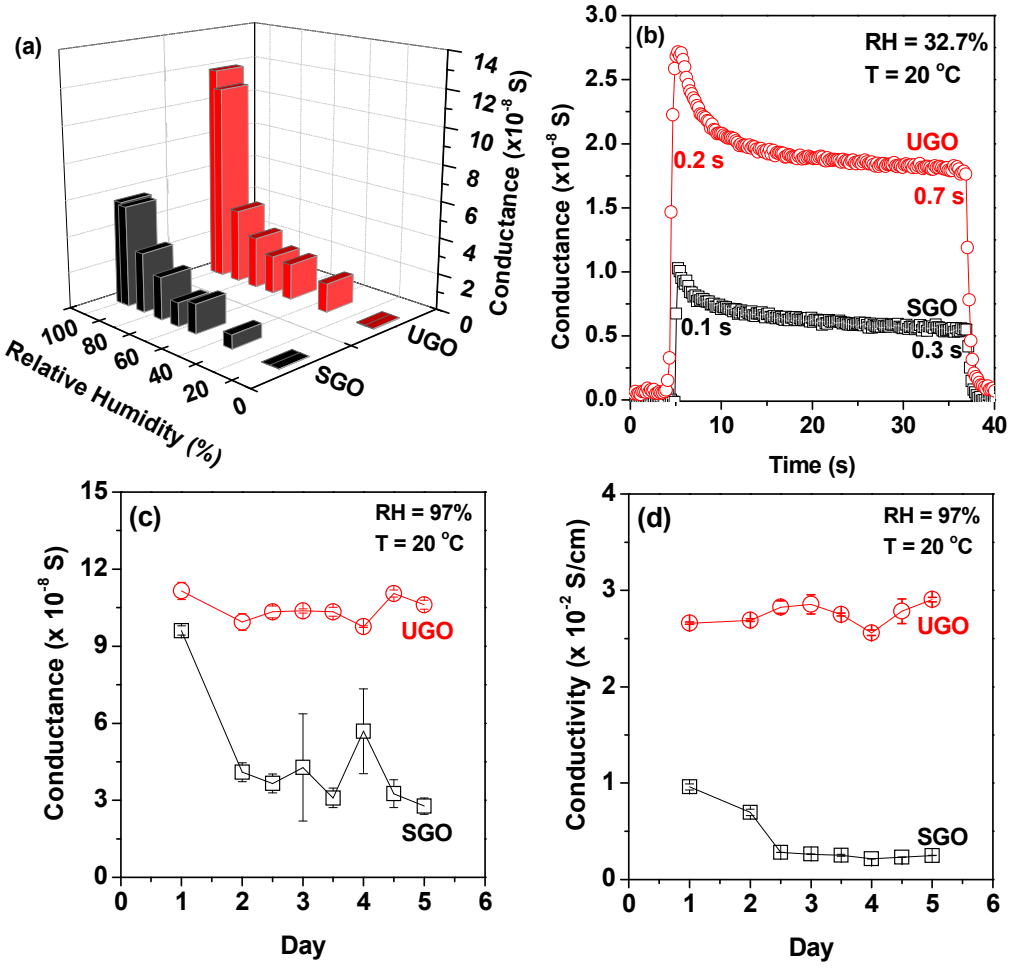

Figure 3. (a) The conductance responses of UGO (red) and SGO (black) films upon exposure to various RH values. (b) The conductance responses of UGO (○) and SGO (□) upon exposure to a modulated humid air flow (32.7 % RH). All measurements were conducted at 20 °C under an applied DC voltage of 1V. The stability study of UGO (○) and SGO (□) humidity sensors was performed by measuring (c) DC conductance and (d) AC conductivity of the devices in a humidity chamber (97 RH%) at 20 °C.

The electrical conductance in GO was understood in terms of the Grotthuss mechanism, which described the proton hopping between H_3O^+ moieties and a freely rotating nearest-neighbour water molecule (Figure S4a).[32,33] Proton transfer along the plane of GO sheets involved rapid exchange of proton through the formation of hydrogen bonding between proton donor (water) and proton acceptor (epoxide or alcohol groups on GO). Therefore, the strength of the hydrogen bond formed between the water molecules and the oxygen functional groups (i.e. epoxide,

hydroxyl and carboxylic acid groups) significantly influenced the proton conduction in GO. Among the oxygenated functional groups (i.e. epoxide, hydroxyl, and carboxylic acid groups) in GO, carboxylic acid group located at edges and boundaries of the GO sheet formed the strongest hydrogen bonds with water molecules.[34] The water molecules strongly bound to the edge of the GO sheet could not contribute to proton conduction.[8,10,13] In fact, an increase in the number of carboxylic moieties at edges of the GO decreased the proton conductivity.[13] The decrease in GO sheet size (as in the case of SGO) increased the number of edges or grain boundaries and, therefore, resulting in higher amount of carboxylic acid groups, which tended to block proton transport pathway (Figure S4b). The net effect was that the overall proton conductivity decreased. Unlike SGO, UGO sheet provided favourable conditions for long-range proton conduction along its large basal plane, which spanned a distance range of ~ 47 to 150 μm (the largest lateral sheet size in UGO). The GO size effects on the overall proton conductivity were apparent in the activation enthalpy (E_a) for proton conduction, measured in the GO sheets. The conductivities of UGO and SGO were determined as a function of temperature (Figure 4a) and were used to plot the respective Arrhenius plots (Figure 4b). As expected, the activation energy for the proton conduction in UGO (E_a = 0.63 eV) was half the value obtained in SGO (E_a = 1.14 eV), supporting the hypothesis that carboxylic acid groups (scattered at the edges and grain boundaries of GO) blocked the in-plane proton conduction.

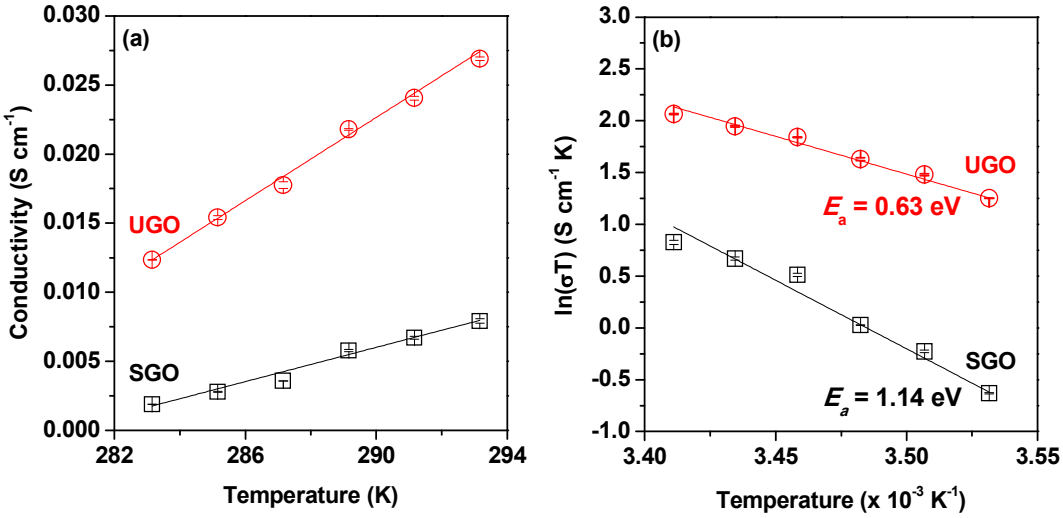

Figure 4. Temperature-dependent conductivities at 97% RH (a) were applied for the Arrhenius plots (b) of UGO (○) and SGO (□), which yielded the activation energies (E_a) of 0.63 eV and 1.14 eV for UGO and SGO, respectively.

3.3 Fingertip Humidity Sensing Properties of UGO Sensor. The UGO electrode was investigated for its utility in the sensing of fingertip moisture, as illustrated in the graphical diagram shown in Figure 5a. The UGO electrode displayed excellent real-time conductance response to the humidity of the fingertip, as the position of the fingertip was withdrawn from the UGO surface (0.5 to 2.5 mm) (Figure 5b). At a fingertip-UGO distance of 0.5 mm, the humidity sensor yielded a sensitivity of 17.4 with extremely fast response/recovery time of 0.6 s/1.3 s (Figure 5c,d). As the fingertip-UGO distance increased from 0.5 to 2.5 mm, the sensitivity and recovery/response time decreased gradually. It should be noted that the fastest response/recovery time (0.4 s/0.7 s) of the UGO humidity sensor was obtained at a fingertip-UGO distance of 2.0 mm. The results of this study indicated that the fingertip humidity sensor based on UGO performed excellently compared to the rGO- and VS_2-based sensors in terms of sensitivity (0.06 for rGO; 3 for VS_2) and response/recovery times (4 s/10 s for rGO; 30 s/12 s for VS_2).[14,35]

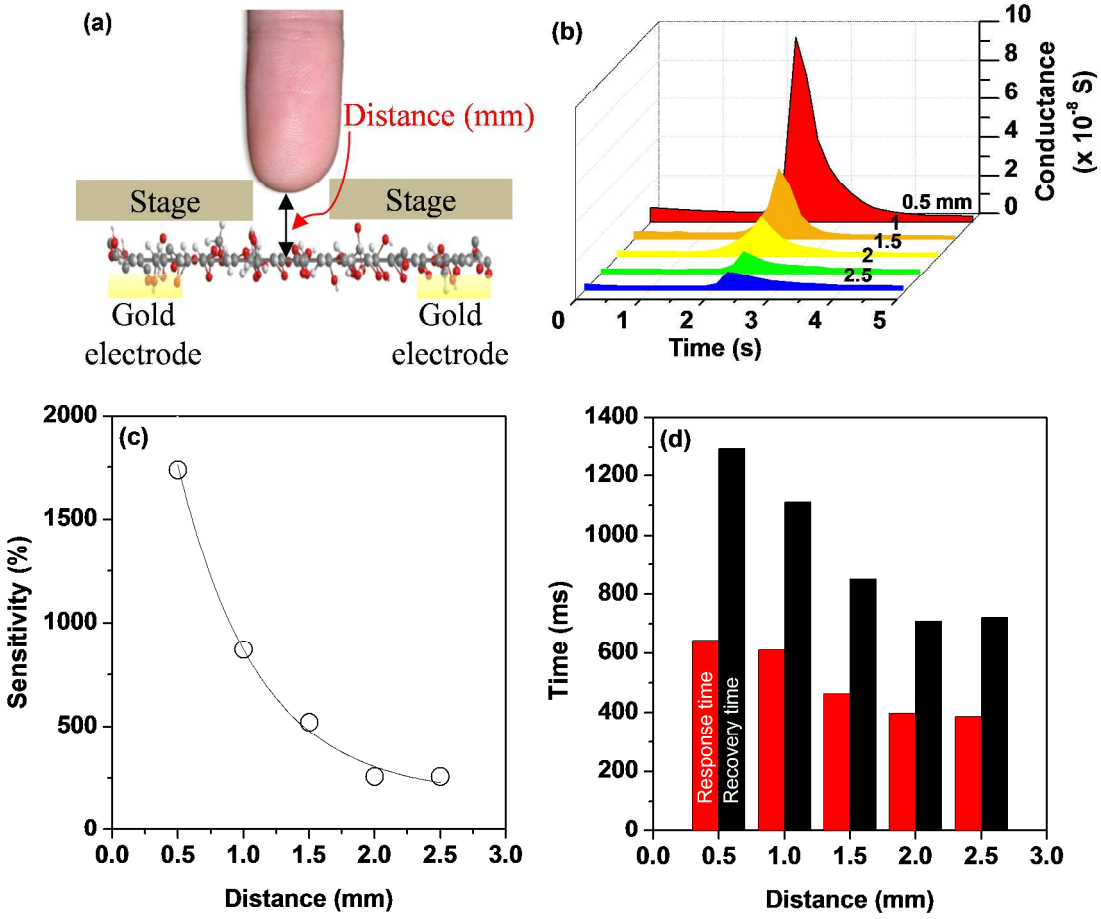

Figure 5. (a) The graphical image of a noncontact-mode UGO humidity sensor responding dynamically to the moisture on a fingertip. A home-made adjustable stage was used to accurately control the fingertip-sensor distance. (b) The conductance changes and (c) the corresponding sensitivity as a function of the distance between the fingertip and the UGO electrode. (d) The response and recovery times of the UGO humidity sensor due to rapid pulse moisture stimuli on the fingertip, which was rapidly either brought forward, or withdrawn from the UGO electrode surface.

4. Conclusion

The graphene oxide particle size was found to influence the humidity sensing performance of a pair of gold electrodes (separated by an inter-electrode gap of 50 μm) drop-coated with either UGO (with a lateral size of 47.4 ± 22.2 μm) or SGO sheets (with a lateral size of 0.8 ± 0.5 μm). As the RH increased from 7 to 100 %, the in-plane conductance of the UGO-coated electrodes increased by four orders of magnitude; whereas the value obtained from the SGO electrodes

increased by three orders of magnitude. The maximal sensitivity values of the UGO and SGO humidity sensors were, therefore, S_{UGO} = 4339 ± 433 and S_{SGO} = 1982 ± 122, indicating the GO size effect on the in-plane conductance. The GO size effects supported the hypothesis that larger GO particles provided favourable conditions for proton conduction along the basal plane due to a reduction in the proton hopping barrier heights (located at the GO intersheets) along the conduction path. The GO size effects on the overall proton conductivity were verified by calculating the activation enthalpy (E_a) required for proton conduction in UGO and SGO sheets. The activation enthalpy for proton conduction in UGO (E_a = 0.63 eV) was half the value measured in SGO (E_a = 1.14 eV). Note that the values of E_a were determined from the Arrhenius plots based on the temperature-dependent conductivities of UGO and SGO electrodes. The UGO humidity sensor exhibited excellent stability with a variation of only ±4.6%, compared to SGO humidity sensor (±48.9%). The sensor stability was evaluated from the DC conductance and the AC conductivity during storage in a humidity chamber (97 % RH, 20 ^{o}C) over 5 days. Interestingly, the response time and recovery time of the humidity sensors did not depend significantly on the GO particle size, and values of 0.2/0.7 s for the UGO electrode and 0.1/0.3 s for the SGO electrode were measured. The use of the resistive-type UGO humidity sensor (operated at a low DC voltage of 1 V) in noncontact-mode humidity sensing showed that the sensor was able to sense the moisture present on a fingertip positioned 0.5 mm away from the sensor with a sensitivity of 17.4 and a response/recovery time of 0.6s/1.3s. The response and recovery times of the UGO electrode were much faster than the corresponding values measured from inorganic vanadium disulfide (VS_2) (response/recovery time = 30 s/12 s).[35] This article highlights the potential utility of UGO in clinical devices including real-time skin moisture

monitor and touchless on/off switch sensor as well as high-speed touchless interaction feature that can be installed directly into a smart phone or smart watch.

Supporting Information Available: Detailed analysis of the UGO and SGO by X-ray photoelectron spectroscopy (XPS) (Figure S5) and Raman Spectroscopy (Figure S6).

Acknowledgements. This research was supported by the Research Grant of Incheon National University in 2015.

References

1. Z. Chen and C. Lu, *Sensor Lett.*, 2005, **3**, 274-295.
2. C. Y. Lee, Lin, C. H., Fu, L. M., in *MEMS/NEMS Handbook Techniques and Applications*, ed. C. T. Leondes, Springer, New York, USA, 2006, vol. 4, ch. 3, p. 63.
3. F. John, in *Sensor Technology Handbook*, ed. J. S. Wilson, Elsevier Inc., Oxford, UK, 2005, ch. 12, p. 271.
4. A. Bagri, C. Mattevi, M. Acik, Y. J. Chabal, M. Chhowalla and V. B. Shenoy, *Nat Chem*, 2010, **2**, 581-587.
5. M. Koinuma, C. Ogata, Y. Kamei, K. Hatakeyama, H. Tateishi, Y. Watanabe, T. Taniguchi, K. Gezuhara, S. Hayami, A. Funatsu, M. Sakata, Y. Kuwahara, S. Kurihara and Y. Matsumoto, *J. Phys. Chem. C*, 2012, **116**, 19822-19827.
6. M. R. Karim, K. Hatakeyama, T. Matsui, H. Takehira, T. Taniguchi, M. Koinuma, Y. Matsumoto, T. Akutagawa, T. Nakamura, S.-i. Noro, T. Yamada, H. Kitagawa and S. Hayami, *J. Am. Chem. Soc.*, 2013, **135**, 8097-8100.
7. S. Ansari, A. Kelarakis, L. Estevez and E. P. Giannelis, *Small*, 2010, **6**, 205-209.
8. R. R. Nair, H. A. Wu, P. N. Jayaram, I. V. Grigorieva and A. K. Geim, *Science*, 2012, **335**, 442-444.

9. R. Hawaldar, P. Merino, M. R. Correia, I. Bdikin, J. Grácio, J. Méndez, J. A. Martín-Gago and M. K. Singh, *Sci. Rep.*, 2012, **2**.

10. A. Buchsteiner, A. Lerf and J. Pieper, *J. Phys. Chem. B*, 2006, **110**, 22328-22338.

11. A. Paneri and S. Moghaddam, *Carbon*, 2015, **86**, 245-255.

12. N. Wei, X. Peng and Z. Xu, *Phys. Rev. E*, 2014, **89**, 012113.

13. K. Hatakeyama, M. R. Karim, C. Ogata, H. Tateishi, A. Funatsu, T. Taniguchi, M. Koinuma, S. Hayami and Y. Matsumoto, *Angew. Chem. Int. Edit.*, 2014, **53**, 6997-7000.

14. X. Wang, Z. Xiong, Z. Liu and T. Zhang, *Adv. Mater.*, 2015, **27**, 1370-1375.

15. I. Jung, D. Dikin, S. Park, W. Cai, S. L. Mielke and R. S. Ruoff, *J. Phys. Chem. C*, 2008, **112**, 20264-20268.

16. T. S. Sreeprasad, A. A. Rodriguez, J. Colston, A. Graham, E. Shishkin, V. Pallem and V. Berry, *Nano Lett.*, 2013, **13**, 1757-1763.

17. A. Ghosh, D. J. Late, L. S. Panchakarla, A. Govindaraj and C. N. R. Rao, *J. Exp. Nanosci.*, 2009, **4**, 313-322.

18. B.-H. Wee and J.-D. Hong, *Adv. Funct. Mater.*, 2013, **23**, 4657-4666.

19. M. Lee, B.-H. Wee and J.-D. Hong, *Adv. Energy Mater.*, 2015, **5**, DOI: 10.1002/aenm.201401890.

20. Q. Zheng, W. H. Ip, X. Lin, N. Yousefi, K. K. Yeung, Z. Li and J.-K. Kim, *ACS Nano*, 2011, **5**, 6039-6051.

21. J. F. Young, *Journal of Applied Chemistry*, 1967, **17**, 241-245.

22. V. C. Tung, M. J. Allen, Y. Yang and R. B. Kaner, *Nat. Nanotechnol.*, 2009, **4**, 25-29.

23. L. J. Cote, F. Kim and J. Huang, *J. Am. Chem. Soc.*, 2008, **131**, 1043-1049.

24. S. Stankovich, D. A. Dikin, G. H. B. Dommett, K. M. Kohlhaas, E. J. Zimney, E. A. Stach, R. D. Piner, S. T. Nguyen and R. S. Ruoff, *Nature*, 2006, **442**, 282-286.

25. K. Erickson, R. Erni, Z. Lee, N. Alem, W. Gannett and A. Zettl, *Adv. Mater.*, 2010, **22**, 4467-4472.

26. J. Jia, C.-M. Kan, X. Lin, X. Shen and J.-K. Kim, *Carbon*, 2014, **77**, 244-254.

27. W. Cai, R. D. Piner, F. J. Stadermann, S. Park, M. A. Shaibat, Y. Ishii, D. Yang, A. Velamakanni, S. J. An, M. Stoller, J. An, D. Chen and R. S. Ruoff, *Science*, 2008, **321**, 1815-1817.

28. D. W. Boukhvalov, M. I. Katsnelson and Y.-W. Son, *Nano Lett.*, 2013, **13**, 3930-3935.

29. X. Shen, X. Lin, N. Yousefi, J. Jia and J.-K. Kim, *Carbon*, 2014, **66**, 84-92.

30. J.-W. Han, B. Kim, J. Li and M. Meyyappan, *J. Phys. Chem. C*, 2012, **116**, 22094-22097.

31. Q. Kuang, C. Lao, Z. L. Wang, Z. Xie and L. Zheng, *J. Am. Chem. Soc.*, 2007, **129**, 6070-6071.

32. K.-D. Kreuer, *Chem. Mater.*, 1996, **8**, 610-641.

33. N. Agmon, *Chem. Phys. Lett.*, 1995, **244**, 456-462.

34. T. Steiner, *Angew. Chem. Int. Edit.*, 2002, **41**, 48-76.

35. J. Feng, L. Peng, C. Wu, X. Sun, S. Hu, C. Lin, J. Dai, J. Yang and Y. Xie, *Adv. Mater.*, 2012, **24**, 1969-1974.

Table of Contents

High-Performance Moisture Sensor based on Ultralarge Graphene Oxide

Boon-Hong Wee,[a] *Wai-Hwa Khoh*,[a] *Ashis K. Sarker*,[b] *Chang-Hee Lee*,[b] *and Jong-Dal Hong*[a]*

[a] Department of Chemistry, Research Institute of Natural Sciences, Incheon National University, 119 Academy-ro, Yeonsu-gu, Incheon, 406-772, Republic of Korea.

[b] Department of Electrical and Computer Engineering, Seoul National University, Seoul 151-742, Republic of Korea

*To whom all correspondence should be addressed.

E-mail: hong5506@inu.ac.kr